



Published in final edited form as:

J Am Chem Soc. 2017 March 15; 139(10): 3647–3650. doi:10.1021/jacs.7b01124.

## Stereocontrolled Synthesis of Kalihinol C

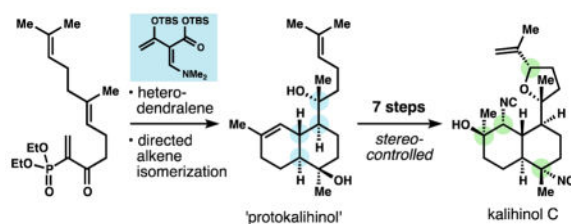
Christopher A. Reiher and Ryan A. Shenvi\*

Department of Chemistry, The Scripps Research Institute, La Jolla, California 92037, United States

### Abstract

We report a concise chemical synthesis of kalihinol C via a possible biosynthetic intermediate, 'protokalihinol,' which was targeted as a scaffold en route to antiplasmodial analogs. High stereocontrol of the kalihinol framework relies on a heterodendralene cascade to establish the target stereotetrad. Common problems of regio- and chemoselectivity encountered in the kalihinol class are explained and solved.

### Graphical Abstract



The kalihinols (Figure 1) possess the highest skeletal and functional group complexity of the biologically-enigmatic isocyanoterpene (ICT) class.<sup>1,2</sup> Kalihinol A<sup>3a</sup> also exhibits the highest reported potency of the ICTs against *P. falciparum*,<sup>3b</sup> killing with an EC<sub>50</sub> of 1 nM, but the mechanism of action has not been rigorously assigned. Proposed mechanisms to explain phenotypic effects of the ICTs include inhibition of heme detoxification<sup>4</sup> or copper chelation,<sup>5</sup> but these proposals do not fully account for the structure-activity relationships and life-cycle activities reported. For example, our discovery that the amphilectenes and adocianes are cytotoxic against liver-stage parasites militates against heme detoxification inhibition as the exclusive antiplasmodial mechanism.<sup>6</sup> Copper *chelation* is simply not possible for congeners with distant isonitriles. As part of a program to investigate the biological activity of ICTs, we have begun to develop effective chemical syntheses<sup>2,6,7</sup> and associated methods<sup>8</sup> to produce and modify three main structural classes: amphilectenes, adocianes, and kalihinols.<sup>1,2</sup> Prior syntheses<sup>9</sup> of the kalihinol class have fought to control stereochemistry in the functionally dense scaffolds, and each contains at least one uncontrolled (*ca.* 1:1 d.r.) stereogenic step.<sup>10</sup> Here we report a short and fully

\*Corresponding Author: rshenvi@scripps.edu.

Supporting Information. Detailed experimental procedures, spectral data, chromatograms and x-ray crystallography. This material is available free of charge via the Internet at <http://pubs.acs.org>.

stereocontrolled synthesis of kalihinol C (**1**) enabled by a new heterodendralene building block, a directed alkene isomerization and a new method for isonitrile synthesis.

The kalihinols appear to derive from a common intermediate, a ‘protokalihinol,’ (**2a**) where the tetrahydrofurans or -pyrans derive from oxidative cyclization of a pendant prenyl unit. The protokalihinol framework (a dihydroxy-bifloran diterpene)<sup>1</sup> would arise from bisaboyl cation intermediate **3** via cation-olefin cyclization and concomitant stereoselective capture of water.<sup>11</sup> While such a pathway might globally simplify formation of the kalihinol stereotetrad (in blue), we thought *intra*-molecular capture of oxygen in synthon **4** might be more realistic than stereoselective carbocation hydration.<sup>12</sup>

Recently, our lab reported short syntheses of amphilectene<sup>7</sup> and adociane<sup>6</sup> ICTs that relied on a new class of polarized dendrimeric polyene<sup>13</sup> (Danishefsky dendralenes) that forges the stereochemically dense core of these and other terpenes<sup>14</sup> in highly diastereoselective Diels-Alder cascades. Given the structural correspondence between amphilectenes and kalihinols, we realized that a dendralene-based approach might emulate the proposed biosynthetic pathway if the oxynucleophile of **4** were embedded in a dendralene.

Short and efficient routes to the heterodendralene and double-dienophile partners are shown in Scheme 1. Preliminary reconnaissance identified two important features of each component. First, the dimethylamine substituent<sup>15</sup> in **5** was necessary to offset the electron-withdrawing carboxylate, which rendered the dendralene less reactive with electron-deficient dienophiles. Second, the diethylphosphonate substituent in **6** activated the dienophile for ambient-temperature cycloaddition but was not so destabilizing as to complicate isolation.

Building block **5** was synthesized by condensation of *tert*-butyl acetoacetate **7** with dimethyl formamide dimethyl acetal (DMF-DMA) to yield vinylogous amide **8**, which was doubly silylated to **5** with loss of the *tert*-butyl group. Geranylphosphonate **6** was also synthesized in two steps by addition of diethyl ethylphosphonate to ethyl geranylacetate (**9**), followed by *in situ* selenation and subsequent oxidation/elimination of the selenoxide.<sup>16</sup>

Cycloaddition of **5** to **6** occurred at 22 °C in CH<sub>2</sub>Cl<sub>2</sub> to yield an inconsequential mixture of diastereomers at the dimethylamino group, which was eliminated to an enone (see synthon **4**) by treatment with hydrogen fluoride. The silylester was also cleaved to the corresponding unsaturated carboxylic acid, which engaged in a nearly quantitative intramolecular Diels-Alder cycloaddition<sup>17</sup> to provide, after tautomerization, β-ketolactone **10**, possessing the targeted stereotetrad of the kalihinols. The stereoisomers (5:1 ratio) corresponded to epimers at the C-P bond, and were converged in the next step.<sup>18</sup>

Lactone **10** was converted to diol **11** by 1. Krapcho-like dephosphonylation, 2. stereoselective methyl addition to the B-ring ketone, and 3. lactone hydrolysis/decarboxylation; each step deserves some comment. First, the desphonylation is a little-precedented transformation that required the development of a new procedure [LiCl, Py•HCl (aq.), 90→110 °C] to spare the acid-sensitive *tert*-alkyl lactone and the electrophilic ketones, which underwent retro-Dieckmann reactions under other conditions. Addition of a methyl group prior to decarboxylation preserved the *trans*-decalin geometry, whereas the

corresponding ketone weakly favored the *cis*-decalin after lactone cleavage. Preferential formation of the *disfavored trans*-decalin (of **11**) has remained unsolved in prior work,<sup>2,9,10</sup> and in this case is enabled by the fused lactone, which locks the geometry. Through this short process, multigram quantities of decalone **11** could be generated in a single pass for elaboration to protokalihinol **2a** and the metabolite itself (**1**).

However, establishment of the required <sup>3,4</sup> unsaturation was undermined by formation of the <sup>4,5</sup> isomer, which predominated upon enolization of ketone **11**. Such preference is well-precedented for 3-decalone enolizations<sup>19</sup> as well as alkene isomerizations in the heavily-studied amorphane sesquiterpenes.<sup>20</sup> Attempts to generate endocyclic alkene **2** by ionization of the tertiary alcohol derived from ketone **11** delivered the isomeric <sup>4,5</sup> alkene with unremitting regularity. Since Brønsted bases can mediate alkene isomerization at high temperatures,<sup>21</sup> we wondered if the tertiary alcohol proximal to the C3 methylene of **11** could mediate a selective alkene isomerization as its strongly basic alkoxide. Indeed, we found that the potassium salt **12** could be heated to 140 °C in DMSO to deliver protokalihinol **2a** with 7:1 selectivity for <sup>3,4</sup> unsaturation (**2**) over <sup>4,5</sup> (**14**, Table 1). Consistent with this mechanistic model, increased equivalents of base led to increased amounts of **14** (entries 1–3), which would derive from *inter*-molecular deprotonation. Small amounts (*ca.* 15%) of isomers derived from chain isomerization ( <sup>15,16</sup>: **2b**, **14b**) also were observed, but could be removed from **2a** (or carried forward and removed from **15**). Other alkali metals besides potassium and other solvents besides DMSO performed poorly (entries 4–5; see SI for a list of other variations). Methods like coordinative isomerization<sup>22</sup> or HAT isomerization<sup>23</sup> (entries 6–7) delivered mixtures of alkenes or the <sup>4,5</sup> isomer exclusively.

A Sharpless-type directed epoxidation<sup>24</sup> was identified as the only method capable of controlling the stereochemistry of the targeted tetrahydrofuran. But to our chagrin, the <sup>3,4</sup> ring-alkene reacted faster than the <sup>14,15</sup> chain-alkene and delivered a C3,4 epoxide opposite to that required for elaboration to the isocyanohydrin of **1** (**16**, see Figure 2). Fortunately, these same conditions also catalyzed a slower, but stereoselective (93:7 d.r.) epoxidation of the side-chain alkene, as well as concomitant 5-*exo*-tet cyclization to the targeted tetrahydrofuran, whereas the A-ring epoxide was spared attack. Consequently, a sodium iodide/zinc metal-mediated epoxide deoxygenation selectively removed the unwanted ring epoxide, whereas the C14,15 oxidation was retained as the incipient hydroxy-tetrahydrofuran (see Figure 2).

The full kalihinol skeleton and correct oxidation state were thus established in eight steps from heterodendralene **5**; we next investigated elaboration to a known metabolite. Elimination of the exocyclic tertiary alcohol was effected by selective trifluoroacetylation and *syn*-elimination via thermolysis since ionizing conditions resulted in hydride shift from the tetrahydrofuran methine. In the same flask, we trifluoroacetylated the remaining alcohol and then installed the A-ring equatorial *tert*-alkyl isonitrile with our solvolytic stereoinversion.<sup>8</sup> The logic leading to this route (Scheme 2) requires some discussion.

We had originally targeted a tandem epoxide opening/trifluoroacetate stereoinversion of **20** (Figure 3) using our solvolysis conditions to install the bis-isonitrile motif. This approach was reported by Vanderwal to be successful, but low-yielding in his kalihinol B synthesis.<sup>9c</sup>

We similarly found that this tandem reaction yielded only small amounts of the bis-isonitrile **21** (5–6%). The basis of the low yield was not the epoxide opening step, which was efficient and regioselective in substrate **20**. Instead, the subsequent B-ring stereoinversion<sup>8</sup> was low-yielding by virtue of competitive elimination (**22**→**23**).<sup>25</sup> Since the epoxide opening occurred faster than trifluoroacetate ionization, and the resulting isocyanohydrin caused elimination in ring B, we concluded that the B-ring C-N bond must be in place prior to epoxidation.

We were dismayed to find that the B-ring functional groups influenced the course of epoxide ionization. As shown in Table 2, the B-ring axial trifluoroacetate and alcohol led to **A** with high selectivity, whereas the equatorial isonitrile or formamide skewed the ratio to favor substantial quantities of regioisomers **B** and **C**, as well as semi-pinacol product **D**.<sup>26</sup> So the A and B-ring substituents proved mutually incompatible in the tandem solvolysis sequence reported by Vanderwal.<sup>9e</sup>

Consequently, we relied on a simple but effective aminolysis to regioselectively generate the requisite A-ring functionality (Scheme 2 and Table 2, entry 5). First, chemoselective oxidation of the alkene of **25** occurred in preference to the isonitrile if carried out with dimethyldioxirane (DMDO) in the strongly hydrogen bond-donating solvent HFIP, which we posit deactivates the isonitrile against oxidation (Scheme 2). Aminolysis in methanol cleanly opened the epoxide to deliver a *sec*-alkyl amino *tert*-alcohol,<sup>27</sup> which was converted to the isocyanohydrin of **1** via difluorocarbene derived from difluoromethyl triflate<sup>28</sup> and KO*t*-Bu. More orthodox methods for amine to isonitrile conversion worked poorly: chloroform/sodium hydroxide<sup>29</sup> generated appreciable amounts of a dichlorocyclopropane and an amide; formylation of the hindered amine occurred slowly due to build up of acid (isonitriles are produced by subsequent formamide dehydration).<sup>30</sup> Our alternative use of difluorocarbene for isonitrile synthesis therefore offers some advantages over existing methods, especially when multiple functional groups are present or the amine is hindered. This three-step procedure provides an efficient, stereo- and chemoselective strategy to install the kalihinol A-ring isocyanohydrin motif.

In summary, we have demonstrated a concise route to access the kalihinol (bifloran) ICTs via a putative biosynthetic inter-mediate, protokalihinol (**2a**) that we anticipate can be divergently advanced to the natural series of metabolites. The synthesis compares favorably to the current best approach to the kalihinols by Vanderwal: it is longer in total step count (17 vs. 12), but higher in yield by an order of magnitude (1.3% vs. 0.13%). The higher efficiency derives from solutions to stereochemical and chemoselectivity problems raised by prior work but left unsolved. Some of these solutions include 1. a method to synthesize the kalihinol stereotetrad using an iterative cycloaddition of the new building block, ‘heterodendralene’ **5**; 2. an alkoxide-directed isomerization method to access the thermodynamically-disfavored<sup>3,4</sup> unsaturated *trans*-bifloran skeleton found throughout the diterpene class, and 3. a short, high-yielding, regio- and stereoselective strategy for installing the A-ring isocyanohydrin motif, including difluorocarbene-mediated isonitrile synthesis. This short and divergent route from protokalihinol **2a** allowed us to generate several analogs related to the metabolite series. We are currently using these compounds to interrogate the antiparasitodal activity and mechanism(s) of the kalihinol class.

## Supplementary Material

Refer to Web version on PubMed Central for supplementary material.

## Acknowledgments

### Funding Sources

Financial support for this work was provided by the NIH (GM105766) and the NSF (GRFP to C. A. R.). Additional support was provided by Eli Lilly, Novartis, Bristol-Myers Squibb, Amgen, Boehringer-Ingelheim, the Sloan Foundation and the Baxter Foundation.

We thank Dr. Milan Gembicky, Dr. Curtis Moore, and Professor Arnold L. Rheingold for X-ray crystallographic analysis. We thank Chris Vanderwal (UC Irvine) for open communication about his ongoing work on the ICTs.

## References

1. Emsermann J, Kahl U, Opatz T. *Mar Drugs*. 2016; 14:16. [PubMed: 26784208]
2. Shenvi RA, Schnermann MJ. *Nat Prod Rep*. 2015; 32:543. [PubMed: 25514696]
3. Isolation: Chang CWJ, Patra A, Roll DM, Scheuer PJ. *J Am Chem Soc*. 1984; 106:4644. kalihinol antimalarial activity: Miyaoka H, Shimomura M, Kimura H, Yamada Y. *Tetrahedron*. 1998; 54:13467.
4. (a) Wright AD, Wang HQ, Gurrath M, Konig GM, Kocak G, Neumann G, Loria P, Foley M, Tilley L. *J Med Chem*. 2001; 44:873. [PubMed: 11300869] (b) Wright AD, McCluskey A, Robertson MJ, MacGregor KA, Gordon CP, Guenther J. *Org Biomol Chem*. 2011; 9:400. [PubMed: 21042642] (c) Young RM, Adendorff MR, Wright AD, Davies-Coleman MT. *Eur J Med Chem*. 2015; 93:373. [PubMed: 25721025]
5. Sandoval IT, Manos EJ, Van Wagoner RM, Delacruz RGC, Edes K, Winge DR, Ireland CM, Jones DA. *Chem Biol*. 2013; 20:753. [PubMed: 23790486]
6. Lu H-H, Pronin SV, Antonova-Koch Y, Meister S, Winzeler EA, Shenvi RA. *J Am Chem Soc*. 2016; 138:7268. [PubMed: 27244042]
7. Pronin SV, Shenvi RA. *J Am Chem Soc*. 2012; 134:19604. [PubMed: 23153381]
8. Pronin SV, Reiher CA, Shenvi RA. *Nature*. 2013; 501:195. [PubMed: 24025839]
9. (a) White RD, Wood JL. *Org Lett*. 2001; 3:1825. [PubMed: 11405721] (b) White RD, Keaney GF, Slown CD, Wood JL. *Org Lett*. 2004; 6:1123. [PubMed: 15040738] (c) Miyaoka H, Abe Y, Sekiya N, Mitome H, Kawashima E. *Chem Commun*. 2012; 48:901. (d) Miyaoka H, Abe Y, Kawashima E. *Chem Pharm Bull*. 2012; 60:1224. [PubMed: 22976335] (e) Daub ME, Prudhomme J, Le Roch K, Vanderwal CD. *J Am Chem Soc*. 2015; 137:4912. [PubMed: 25815413] (f) Daub ME, Prudhomme J, Mamoun CB, Le Roch KG, Vanderwal CD. *ACS Med Chem Lett*.
10. Kalihinene X was synthesized with stereocontrol in 35-steps, but lacks the A-ring isocyanohydrin and characteristic *trans*-ring fusion of the kalihinols. See: Miyaoka H, Shida H, Yamada N, Mitome H, Yamada Y. *Tetrahedron Lett*. 2002; 43:2227.
11. Dewick, PM. *Medicinal Natural Products: A Biosynthetic Approach*. Wiley; 2009.
12. For an exception, see: Zhao C, Toste FD, Raymond KN, Bergman RG. *J Am Chem Soc*. 2014; 136:14409. [PubMed: 25265509]
13. For an excellent review of dendralenes, see: Hopf H, Sherburn MS. *Angew Chem Int Ed*. 2012; 51:2298.
14. Newton CG, Drew SL, Lawrence AL, Willis AC, Paddon-Row MN, Sherburn MS. *Nat Chem*. 2015; 7:82. [PubMed: 25515894]
15. Kozmin SA, Rawal VH. *J Org Chem*. 1997; 62:5252–5253.
16. Reich HJ, Renga JM, Reich IL. *J Org Chem*. 1975; 97:5434.
17. For the closest precedent to this stereoselective cycloaddition, see: Tietze LF, Beifuss U, Ruther M. *J Org Chem*. 1989; 54:3120.

18. The diastereomers of 10 could also be separated and shown to converge to the same product upon dephosphonylation.
19. Huffman JW, Balke WH. *J Org Chem.* 1988; 53:3828.
20. Ngo K, Brown GD. *Tetrahedron.* 1999; 55:15109.
21. Schriesheim A, Muller RJ, Rowe CA. *J Am Chem Soc.* 1962; 84:3164.
22. Harrod JF, Chalk AJ. *J Am Chem Soc.* 1964; 86:1776.
23. Crossley SWM, Barabé F, Shenvi RA. *J Am Chem Soc.* 2014; 136:16788. [PubMed: 25398144]
24. Nicolaou KC, Harrison ST. *Angew Chem Int Ed.* 2006; 45:3256.
25. Stereoselectivity was also poor and the remaining material could not be identified. See Ref ixf.
26. Stereochemistry depicted assumes a thermally-allowed 2-electron suprafacial Wagner-Meerwein shift.
27. Wood accesses a related amino alcohol (Ref. ixb) by epoxide-opening with  $\text{NaN}_3$ , followed by  $\text{Na}^0$  reduction, conditions which are reported to reduce isonitriles.
28. (a) Fier PS, Hartwig JF. *Angew Chem Int Ed.* 2013; 52:2092.(b) Levin VV, Dilman AD, Belyakov PA, Struchkova MI, Tartakovsky VA. *J Fluorine Chem.* 2009; 130:667.
29. (a) Hofmann AW. *Ann.* 1868; 298:202.(b) Sasaki T, Eguchi S, Katada T. *J Org Chem.* 1974; 39:1239.
30. Hertler WR, Corey EJ. *J Org Chem.* 1958; 23:1221.

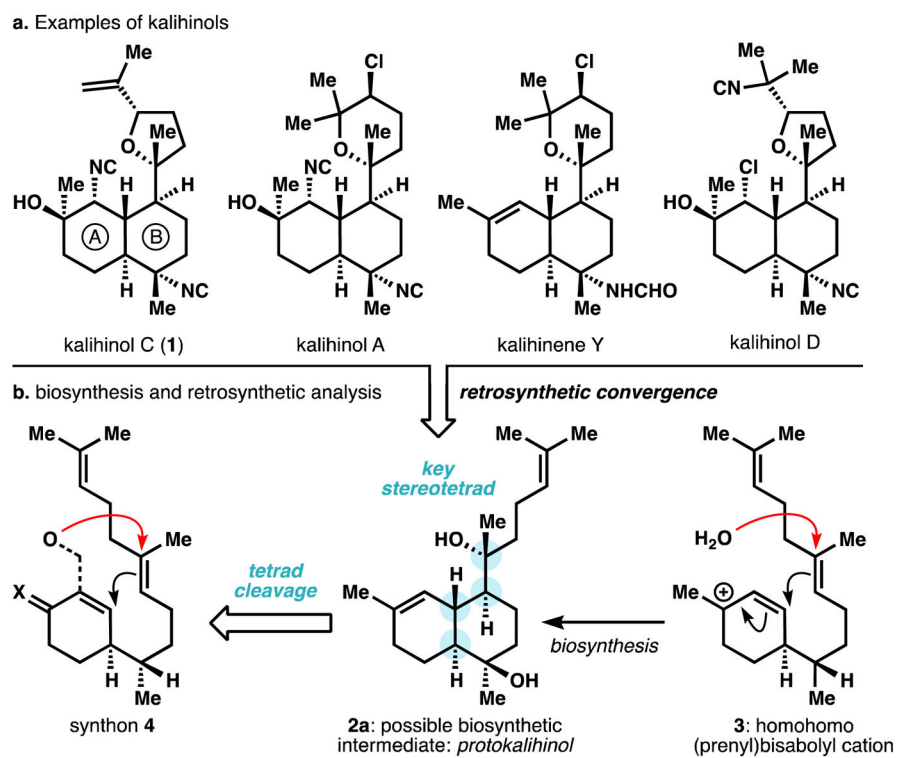


**Figure 1.**  
**a.** Kalihinol congeners **b.** hypothetical biosynthesis that informs a proposed chemical synthesis.

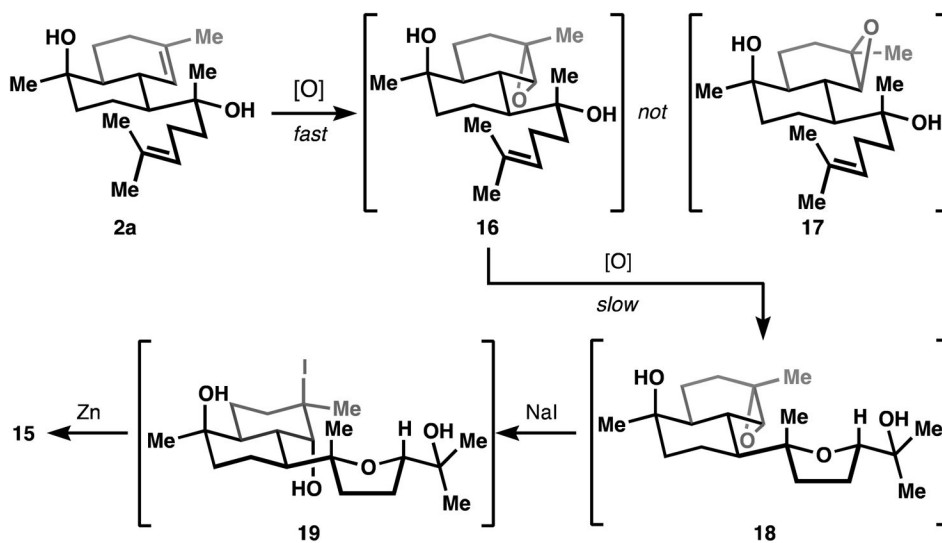
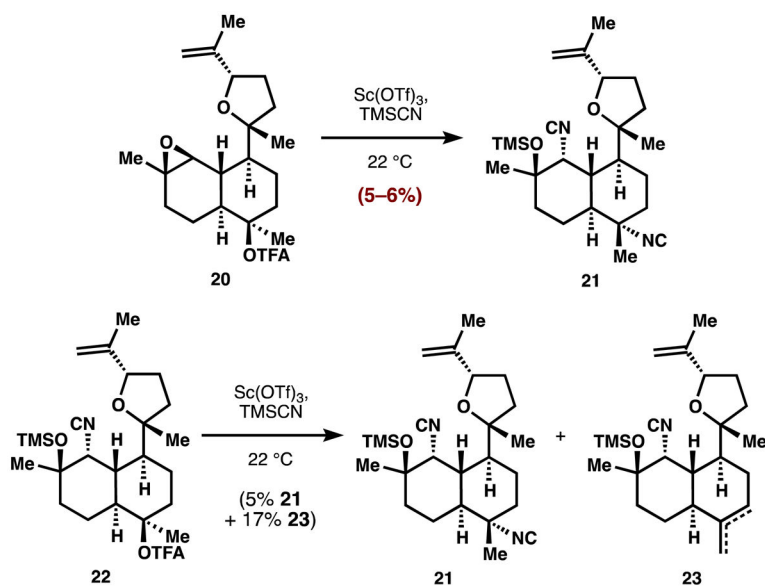
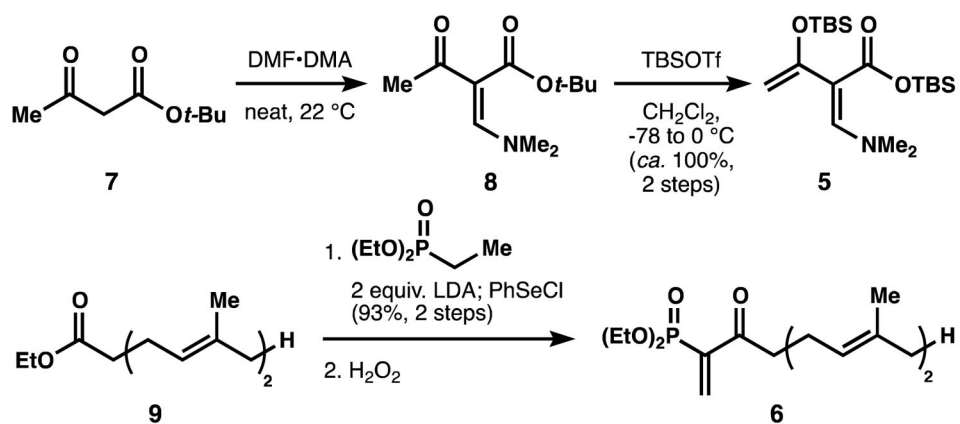


Figure 2.  
Stereoselective oxidative cyclization to 15.

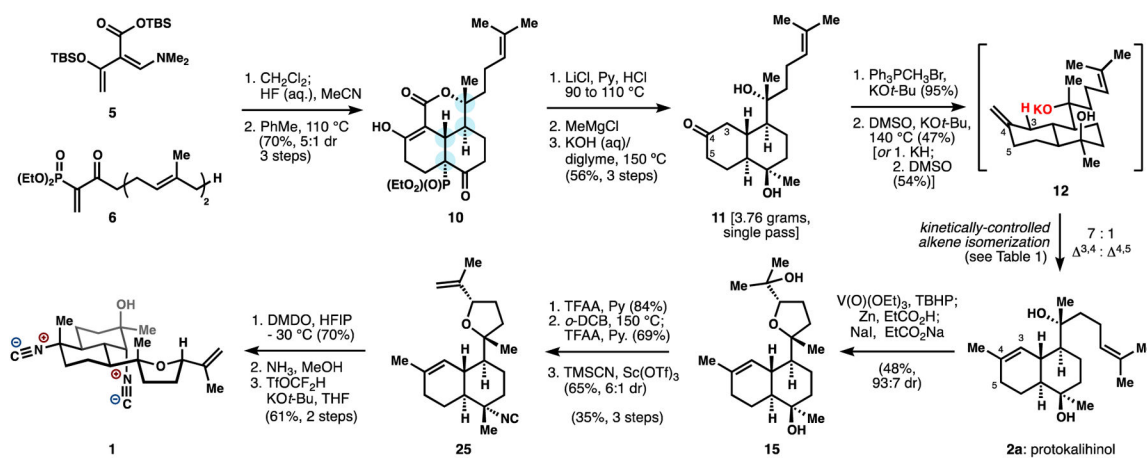




**Figure 3.**  
Tandem isonitrile formation is very low yielding.



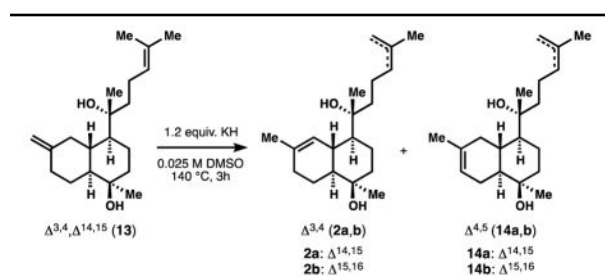
**Scheme 1.**  
Routes to building blocks.



**Scheme 2.**  
Synthesis of kalihinol C.

Table 1

Alkoxide-directed alkene isomerization.



Entry	Variations (& % conversion)	2:14	%2a
1	none (78)	7:1	54
2 <sup>a</sup>	4 equiv. KO <sup>t</sup> Bu, no KH (82)	5:1	55
3 <sup>a</sup>	16 equiv. KO <sup>t</sup> Bu, no KH (86)	1:1	28
4	1.2 equiv. <i>n</i> -BuLi, no KH (0)	–	0
5	DMPU instead of DMSO (0)	–	0
Alternate Conditions			
6 <sup>b</sup>	20 mol% RhCl <sub>3</sub> , EtOH/H <sub>2</sub> O, 70 °C (56)	1:1	28
7 <sup>a</sup>	2 mol% [Co], <sup>c</sup> 4 mol% PhSiH <sub>3</sub> , PhH (42)	<1:20	<5

<sup>a</sup><sub>1</sub>H NMR;<sup>b</sup> GCMS;<sup>c</sup>Co(Sal<sup>*t*</sup>-Bu,<sup>*t*</sup>-Bu)Cl•H<sub>2</sub>O

Table 2

Isocyanohydrin installation.<sup>a</sup>

R <sup>1</sup> / R <sup>2</sup>	Conditions [N]	R <sup>1</sup> / R <sup>2</sup>	A:B:C:D
<b>OTFA / Me</b>	TMSCN, Sc(OTf) <sub>3</sub> [NC]	<b>OTFA / Me</b>	83:0:17:0
<b>OH / Me</b>	TMSCN, Sc(OTf) <sub>3</sub> [NC]	<b>OTMS / Me</b>	100:0:0:0
<b>Me / NC</b>	TMSCN, Sc(OTf) <sub>3</sub> [NC]	<b>Me / NC</b>	61:0:39:0
<b>Me / NHCHO</b>	TMSCN, Sc(OTf) <sub>3</sub> [NC]	<b>Me / NHCHO</b>	54:31:15:0
<b>Me / NC</b>	NH <sub>3</sub> , MeOH [NH <sub>2</sub> ]	<b>Me / NC</b>	100:0:0:0

<sup>a</sup> Any silylethers were converted to alcohols with TBAF.